universe

IMPACT FACTOR 2.5

CITESCORE 4.3

Article

Probing Dark Photons Through Gravitational Decoupling of Mass-State Oscillations in Interstellar Media

Bo Zhang and Cui-Bai Luo

Special Issue

Universe: Feature Papers 2024—"Galaxies and Clusters"

Edited by

Prof. Dr. Mauro D'Onofrio

MDPI

https://doi.org/10.3390/universe11040115

universe

MDPI

Article

Probing Dark Photons Through Gravitational Decoupling of Mass-State Oscillations in Interstellar Media

Bo Zhang and Cui-Bai Luo *

Department of Physics, Anhui Normal University, Wuhu 241002, China; bo_zhang_work@163.com
* Correspondence: cuibailuo@ahnu.edu.cn

Abstract: We propose a novel mechanism for photon–dark photon mass-state oscillations mediated by gravitational separation during propagation through the interstellar medium. This phenomenon establishes a new avenue for the detection of dark matter. By analyzing gravitational lensing data from quasars, we investigate the sensitivity of this approach to dark photons. Our analysis demonstrates constraints of $\varepsilon < 10^{-2}$ in the dark photon mass range of 1.7×10^{-14} eV to 5.4×10^{-14} eV. Furthermore, we propose potential applications of this mechanism to astrophysical systems with strong gravitational fields, such as neutron stars and black hole accretion disks.

Keywords: dark photon detection; dark matter; gravitational lensing

check for updates

Academic Editors: Mauro D'Onofrio and Andrea Lapi

Received: 4 February 2025
Revised: 12 March 2025
Accepted: 25 March 2025
Published: 1 April 2025

Citation: Zhang, B.; Luo, C.-B. Probing Dark Photons Through Gravitational Decoupling of Mass-State Oscillations in Interstellar Media. *Universe* **2025**, *11*, 115. https://doi.org/10.3390/universe11040115

1. Introduction

The Standard Model (SM) has achieved remarkable success over the past decades, yet persistent observational anomalies—including cosmic-ray excesses like the AMS-02 positron anomaly [1]—strongly motivate extensions beyond its framework. To address these discrepancies, numerous beyond-the-Standard-Model (BSM) theories have been proposed. The minimal extension involves the introduction of an additional $U(1)_{\mathrm{h}}$ gauge symmetry [2], which may emerge as a low-energy effective theory of ultraviolet-complete models [3–5]. This symmetry naturally predicts a new gauge boson, termed the dark photon X_μ, that kinetically mixes with the Standard Model photon X_μ. The corresponding extended Lagrangian is as follows [6]:

$$L_K = -\frac{1}{4}F^{\mu\nu}F_{\mu\nu} - \frac{1}{4}X^{\mu\nu}X_{\mu\nu} + \frac{\sin\chi_0}{2}X^{\mu\nu}F_{\mu\nu} + \frac{m_\chi^2}{2}cos^2\chi_0 X_\mu X^\mu - eA_\mu J^\mu_{\mathrm{em}}, \quad (1)$$

where $F^{\mu\nu} = \partial^\mu A^\nu - \partial^\nu A^\mu$ and $X^{\mu\nu} = \partial^\mu X^\nu - \partial^\nu X^\mu$ denote the field strength tensors of the photon and dark photon fields, respectively. Here, m_χ represents the dark photon mass, J^μ_{em} is the electromagnetic current, and χ_0 is the mixing angle.

During propagation through a medium, the photon–dark photon interaction states undergo oscillations. For transversely polarized photons, the oscillation probability is given by [7,8]

$$P = \varepsilon^2 \frac{m_\chi^4}{|m_\gamma^2 - m_\chi^2|^2}, \quad (2)$$

where m_γ denotes the effective photon mass within the medium and ε represents the kinetic-mixing parameter, which associates with χ_0. In the sub-MeV mass regime ($m_\chi < 1$ MeV), this oscillation mechanism underpins key dark photon detection strategies, including cosmic microwave background (CMB) analyses [9–12], "light-shining-through-wall" experiments (LSW) [13], helioscopes experiments [4], and direct detection efforts [14,15].

Equation (2) reveals that when $m_\chi \ll m_\gamma$, the oscillation probability becomes suppressed as $P \propto (m_\chi/m_\gamma)^4$. Consequently, the sensitivity of these experiments is fundamentally limited by the medium's effective photon mass m_γ.

Gravitational lensing serves as a powerful tool for testing general relativity [16–18], searching for compact objects [19–21], and other astrophysical applications. In neutrino systems analogous to the dark photon scenario, gravitational lensing has been utilized to determine neutrino mass ordering [22]. J.F. Glicenstein [23] investigated coherent and incoherent gravitational lensing phenomena in photon–dark photon systems, akin to observations of active galactic nucleus (AGN) radio wavebands deflected by the Sun [24], discussing time-delay signatures.

In this work, we propose a novel mechanism leveraging gravitationally induced decoupling of photon–dark photon mass eigenstates during propagation. We derive the oscillation probability between these mass states in gravitational fields, which could addresses the medium-induced suppression of oscillations at ultralow dark photon masses, thereby offering a new paradigm for dark photon detection. By modeling gravitational dispersion effects in gravitationally lensed quasar systems, we demonstrate that photon-to-dark-photon oscillations reduce the apparent luminosity of these astrophysical sources. Our calculations indicate that this approach achieves sensitivity to the kinetic-mixing parameter $\varepsilon < 10^{-2}$ for dark photon masses near 10^{-14} eV.

In Section 2, we derive the oscillation probability for photon–dark photon mass eigenstates propagating through a medium in gravitational fields. Section 3 investigates the suppression of apparent flux in gravitationally lensed quasars induced by the oscillations mechanism. Section 4 quantifies the sensitivity of this method, using characteristic scales. Finally, we conclude by summarizing our results and proposing extensions of this framework to probe the oscillation in strong gravitational environments, such as neutron stars and black holes.

2. The Oscillation Model

The dark photon Lagrangian given in Equation (1) contains the kinetic mixing term $X^{\mu\nu}F_{\mu\nu}$. Through the field redefinition $A, X \to A_{\mathrm{R}}, S$, the mixing term can be diagonalized:

$$\begin{aligned} L_{\mathrm{I}} = & -\frac{1}{4}A_{\mathrm{R}\mu\nu}^2 - \frac{J_{\mathrm{em}}^\mu}{\cos\chi_0}A_{R\mu} - \frac{1}{4}S_{\mu\nu}^2 \\ & + \frac{1}{2}(A_{\mathrm{R}\mu}S_\mu)\begin{bmatrix} m_\chi^2\sin^2\chi_0 & m_\chi^2\cos\chi_0\sin\chi_0 \\ m_\chi^2\cos\chi_0\sin\chi_0 & m_\chi^2\cos^2\chi_0 \end{bmatrix}\begin{pmatrix} A_{\mathrm{R}\mu} \\ S_\mu \end{pmatrix}, \end{aligned} \tag{3}$$

where

$$\begin{aligned} A_{\mathrm{R}} &= \cos\chi_0 A \\ S &= X - \sin\chi_0 A. \end{aligned} \tag{4}$$

In the Lagrangian L_{I} (3), the photon and the additional boson are kinetically decoupled, with $A_{\mathrm{R}\mu}$ interacting directly with the electromagnetic current. Consequently, $A_{\mathrm{R}\mu}$ represents the physically observable photon field in the dark photon model, while S corresponds to the sterile component, i.e., the dark photon field.

In vacuum ($J_{\mathrm{em}}^\mu = 0$), the mass matrix in L_{I} is diagonalized via the unitary transformation $U_{\mathrm{I}\to\mathrm{m}}$:

$$U_{\mathrm{I}\to\mathrm{m}} = \begin{bmatrix} \cos\chi_0 & -\sin\chi_0 \\ \sin\chi_0 & \cos\chi_0 \end{bmatrix}, \tag{5}$$

yielding the diagonalized Lagrangian:

$$L_{\mathrm{m}} = -\frac{1}{4}A_{1\mu\nu}^2 - \frac{1}{4}A_{2\mu\nu}^2 + \frac{1}{2}(A_1^\mu A_2^\mu)\begin{bmatrix} 0 & 0 \\ 0 & m_\chi^2 \end{bmatrix}\begin{pmatrix} A_{1\mu} \\ A_{2\mu} \end{pmatrix}. \tag{6}$$

The kinetic terms for A_1 and A_2 are fully diagonal, with masses 0 and m_χ, respectively. Therefore, A_1 and A_2 are the mass eigenstates for vacuum propagation, related to the interaction states $(A_{\mathrm{R}\mu}, S)$ via the transformation matrix $U_{\mathrm{I}\to\mathrm{m}}$:

$$\begin{pmatrix} A_{1\mu} \\ A_{2\mu} \end{pmatrix} = U_{\mathrm{I}\to\mathrm{m}} \cdot \begin{pmatrix} A_{\mathrm{R}\mu} \\ S_\mu \end{pmatrix}. \tag{7}$$

In a medium, photon propagation is governed by the medium's properties. Classical electrodynamics attributes this to a complex effective photon mass $\bar{m}_\gamma$. The electromagnetic current in the Lagrangian is then

$$J_{\mathrm{em}}^\mu = \frac{\bar{m}_\gamma^2}{2}A_{\mathrm{R}}^\mu. \tag{8}$$

The real part of the complex effective mass represents forward coherent scattering by medium particles, while the imaginary part accounts for photon absorption by the medium. Specifically,

$$\bar{m}_\gamma^2 = m_\gamma^2 + iE_\gamma\Gamma \tag{9}$$

where m_γ is the real effective photon mass, E_γ denotes the photon energy, and $1/\Gamma$ corresponds to the optical depth of photons in the medium.

Substitution into L_{I} (Equation (3)) enables diagonalization of the mass matrix through the field rotation $U_{\mathrm{I}\to\mathrm{M}}$:

$$U_{\mathrm{I}\to\mathrm{M}} = \begin{pmatrix} \cos\chi_0 & -\frac{\sin\chi_0 m_\chi^2}{m_\chi^2 - \bar{m}_\gamma^2} \\ \frac{\sin\chi_0 m_\chi^2}{m_\chi^2 - \bar{m}_\gamma^2} & \cos\chi_0 \end{pmatrix}. \tag{10}$$

The diagonalized Lagrangian becomes

$$L_{\mathrm{M}} = -\frac{1}{4}M_{1\mu\nu}^2 - \frac{1}{4}M_{2\mu\nu}^2 + \frac{1}{2}(M_1^\mu M_2^\mu)\begin{bmatrix} \bar{m}_\gamma^2 + \frac{m_\chi^2\bar{m}_\gamma^2\sin^2\chi_0}{m_\chi^2} & 0 \\ 0 & \bar{m}_\gamma^2 - \frac{m_\chi^2\bar{m}_\gamma^2\sin^2\chi_0}{m_\chi^2} \end{bmatrix}\begin{pmatrix} M_{1\mu} \\ M_{2\mu} \end{pmatrix}, \tag{11}$$

where M_1 and M_2 are medium-dependent eigenstates with diagonal kinetic and mass terms. These eigenstates relate to the interaction basis $(A_{\mathrm{R}\mu}, S)$ via

$$\begin{pmatrix} M_{1\mu} \\ M_{2\mu} \end{pmatrix} = U_{I\to M} \cdot \begin{pmatrix} A_{R\mu} \\ S_\mu \end{pmatrix}. \tag{12}$$

We analyze photon propagation through the interstellar medium in gravitational fields and calculate the oscillation probabilities between mass eigenstates. The medium-dependent eigenstates (M_1, M_2) and vacuum mass eigenstates (A_1, A_2) are connected via the unitary rotation matrix:

$$U_{\mathrm{M}\to\mathrm{m}} = U_{\mathrm{I}\to\mathrm{m}}U_{\mathrm{I}\to\mathrm{M}}^{-1}, \tag{13}$$

where $U_{\mathrm{I}\to\mathrm{m}}$ and $U_{\mathrm{I}\to\mathrm{M}}$ are defined in Equations (5) and (10). For a system initially in the mass eigenstates $(A_1(0), A_2(0))$, its time evolution follows

$$\begin{pmatrix} A_1(t) \\ A_2(t) \end{pmatrix} = U_{\mathrm{M}\to\mathrm{m}} e^{-iHt} U^{-1}_{\mathrm{M}\to\mathrm{m}} \begin{pmatrix} A_1(0) \\ A_2(0) \end{pmatrix}, \tag{14}$$

with H being the diagonalized Hamiltonian. Photons emitted in the $(1,0)$ state (pure A_1) oscillate to A_2 with probability

$$P_{A_1\to A_2} = \sin^2 2\chi_0 \frac{|\bar{m}^2_\gamma|^2}{|m^2_\chi - \bar{m}^2_\gamma|^2} \sin^2\left(\frac{(m^2_\chi - m^2_\gamma)t}{4E_\gamma}\right). \tag{15}$$

For astrophysical (incoherent) sources, the oscillatory term $\sin^2(\cdot)$ averages to $1/2$. Defining the mixing parameter $\varepsilon = \sqrt{2}\sin\chi_0$, the effective probability becomes

$$P_{A_1\to A_2} = \varepsilon^2 \frac{m^4_\gamma + (E_\gamma\Gamma)^2}{(m^2_\chi - m^2_\gamma)^2 + (E_\gamma\Gamma)^2}. \tag{16}$$

Equation (16) provides the oscillation probability between photon and dark photon mass states in a medium under weak external gravitational fields. Crucially, this result diverges from the interaction states oscillation probability (Equation (2)) derived for media. In the regime $m_\chi \ll m_\gamma$, where the dark photon mass is significantly smaller than the medium's effective photon mass, the mass-state oscillation probability remains unsuppressed. This advantage is expected to be applied in detection experiments.

3. Example of Gravitational Lensing Quasar Scheme

Under gravitational field effects, mass eigenstates (A_1, A_2) propagating along spacetime geodesics experience differential trajectory shifts (geodesic deviations), inducing decoherence between the eigenstates. Remarkably, gravitational fields can mimic the decoherence effects traditionally attributed to absorptive media—such as reactor core plasma [7,25] or solar plasma in helioscope experiments [4,26]—but with a critical distinction; absorptive media suppress oscillations by decohering interaction eigenstates (A_R, S), while gravitational fields decohere mass eigenstates (A_1, A_2) through spacetime curvature gradients.

Figure 1 schematically illustrates the astrophysical system under study. Photons emitted from a distant quasar are gravitationally deflected by a foreground galaxy and detected by observers. In the dark photon framework, medium-induced oscillations between the mass eigenstates (A_1, A_2) occur during propagation through the interstellar medium. Simultaneously, the foreground galaxy's gravitational field induces geodesic separation between the eigenstates (black dashed line). This dual effect modifies the quasar's apparent flux and introduces spectral distortions.

By analyzing flux discrepancies in gravitationally lensed quasars—compared to unlensed counterparts—we derive constraints on the dark photon parameter space. In this section, we formulate the flux suppression caused by photon–dark photon oscillations in lensed systems, providing a quantitative tool for such analyses.

Consider a flux of N_0 photons propagating through the galactic medium. Decoherence between mass eigenstates arises over a characteristic distance l due to gravitational geodesic deviation. The photon attenuation follows

$$dN = -N\frac{P(z)}{l} dL(z), \tag{17}$$

where P is the oscillation probability between mass eigenstates, etc., as shown in Equation (16). It is particularly important to note that the oscillation probability P is a function of redshift. Since m_γ itself depends on redshift, it can be expressed as [9]

$$\begin{aligned} m_\gamma^2(z) &\approx 1.4 * 10^{-21} \left(\frac{n_\mathrm{p}(z)}{cm^3}\right) eV^2 \\ n_\mathrm{p}(z) &= (1 - \tfrac{Y_\mathrm{p}}{2}) \eta \tfrac{2\zeta(3)}{\pi^2} T_0^3 (1+z)^3 \end{aligned} \tag{18}$$

where $n_\mathrm{p}(z)$ is the density of the proton, $Y_\mathrm{p} = 0.25$, $\eta = 6.7 \times 10^{-10}$, $\zeta(3)$ is the Riemann zeta function, $T_0 = 2.725$ K is the current temperature of the CMB, and z denotes the redshift of the interstellar medium. In the subsequent discussion, we will consider photons of optical energy scale (eV) propagating through the interstellar medium. In this regime, the optical depth is dominated by photon–electron Thomson scattering, expressed as

$$\Gamma(z) = n_e(z) \cdot \sigma_\mathrm{T} \tag{19}$$

where $\sigma_\mathrm{T} = 6.65 \times 10^{-25}$ cm^2 is the Thomson scattering cross-section and $n_\mathrm{e}(z)$ denotes the electron density. For redshifts $z < 1$, the hydrogen ionization fraction is $X_\mathrm{e}(z) = n_\mathrm{e}(z)/n_\mathrm{p}(z) \approx 1$, thus implying $n_\mathrm{e}(z) \approx n_\mathrm{p}(z)$. The conversion between luminosity distance L and redshift is given by

$$L(z) = \frac{(1+z)}{H_0} \int_0^z \frac{dz'}{\sqrt{\Omega_\mathrm{m}(1+z')^3 + \Omega_\Lambda}} \tag{20}$$

with $\Omega_\mathrm{m} = 0.3, \Omega_\Lambda = 0.7$, and H_0 representing the current Hubble constant. Integrating Equation (17) gives

$$N = N_0 \exp\left(-\int P(L) \frac{dL}{l}\right) = N_0 \exp\left(-\int P d\tau\right), \tag{21}$$

where $d\tau \equiv dL/l$ represents the average number of times, $d\tau$, that the photon mass states undergo decoherence after propagating a distance dL. The attenuation factor N/N_0 corresponds to the observed quasar luminosity suppression.

To estimate τ, we compute the differential angular deflection $\Delta\alpha$ between photons and dark photons using weak-field general relativity:

$$\Delta\alpha = \frac{2GM}{R_\mathrm{gal} c^2} \left(\frac{m_\chi^2}{E_\gamma^2 - m_\chi^2}\right). \tag{22}$$

Here, R_gal is the characteristic scale of the gravitational lens, and the full derivation is given in Appendix A.

The maximum path-length difference between photons and dark photons L_h, induced by their differential deflection, is approximated as

$$L_\mathrm{h} \approx L_\mathrm{s} \times \Delta\alpha, \tag{23}$$

where L_s is the quasar–Earth distance. For a photon energy E, the coherence length of the thermal photon wavepacket is [27]

$$\Delta h = \frac{197\mathrm{MeV} \cdot \mathrm{fm}}{E_\gamma}, \tag{24}$$

which corresponds to the de Broglie wavelength scale. While the actual propagation paths include non-geodesic corrections, the sub-eV dark photon mass ensures minimal trajectory separation, justifying a linearized approximation for the optical depth:

$$d\tau = \frac{dL_{\mathrm{h}}}{\Delta h} = dL_{\mathrm{s}} \frac{\Delta \alpha}{\Delta h}. \tag{25}$$

From Equation (20), the differential relation of dL_{s} and dz satisfies

$$dL_{\mathrm{s}} = \left[\frac{1}{H_0} \int_0^z \frac{dz'}{\sqrt{\Omega_{\mathrm{m}}(1+z')^3 + \Omega_\Lambda}} + \frac{1+z}{H_0 \sqrt{\Omega_{\mathrm{m}}(1+z)^3 + \Omega_\Lambda}} \right] dz \tag{26}$$

Substituting Equations (22)–(25) into Equation (21), the quasar's flux suppression becomes

$$\frac{N}{N_0} \approx 1 - \frac{E}{197\mathrm{MeV} \cdot \mathrm{fm}} \frac{2GM}{R_{\mathrm{gal}} c^2} \left(\frac{m_\chi^2}{E_\gamma^2 - m_\chi^2} \right) \int dL_{\mathrm{s}}(z) \frac{\varepsilon^2 (m_\gamma^4(z) + (E_\gamma \Gamma(z))^2)}{(m_\chi^2 - m_\gamma^2(z))^2 + (E_\gamma \Gamma(z))^2}. \tag{27}$$

The $1/(E_\gamma^2 - m_\chi^2)$ dependence in Equation (27) indicates stronger attenuation at lower photon energies ($E_\gamma \gg m_\chi$), leading to spectral hardening.

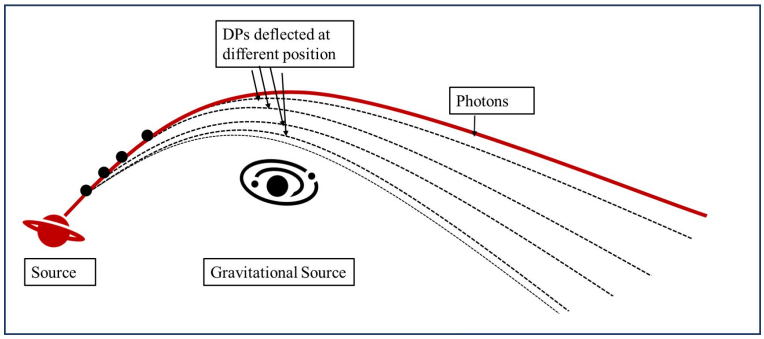

Figure 1. Illustration of this detection mechanism in a gravitationally lensed quasar system. Photons (red solid line) emitted from the quasar follow bent geodesics due to the foreground galaxy's gravitational potential. The oscillated dark photon component (black dashed line) propagates along a distinct path, with the spatial separation between mass eigenstates suppressing quantum interference.

4. Results and Discussions

The quasar luminosity function quantifies the number density of quasars as a function of intrinsic brightness and redshift [28–30]. By analyzing redshift-binned luminosity distributions, the cosmological evolution of quasar populations can be reconstructed [31]. We extend this framework to gravitationally lensed quasars, comparing their luminosity function with unlensed populations. Gravitational lensing-induced chromatic dispersion—arising from photon–dark photon oscillations—suppresses the observed flux of lensed quasars.

A statistically significant signature emerges when the flux attenuation exceeds an assumed threshold of 10% ($N/N_0 < 0.1$), which we conservatively adopt based on instrumental sensitivity limits and astrophysical background uncertainties in current surveys.

We adopt typical parameters for quasar gravitational lensing systems: a source redshift $z = 1$ (comoving distance L_{s}), a foreground galaxy radius $R_{\mathrm{gal}} = 1$ kpc, and a galaxy mass $M = 10^{12} M_\odot$. The analysis assumes optical wavelength observations ($E_\gamma \sim$ eV).

As shown in the Figure 2, our proposed scheme achieves a sensitivity on the order of 10^{-2} for dark photon masses in the range 1.7×10^{-14} eV to 5.4×10^{-14} eV. Notably, within this region, there exist multiple peaks of significantly enhanced sensitivity, reaching 10^{-5}. This arises from a resonance phenomenon caused by the matching of the dark photon

mass with the effective photon mass in the medium, as demonstrated in Equation (27). Similar features have been observed in the constraints derived from broadband radio spectra of compact radio sources [32].

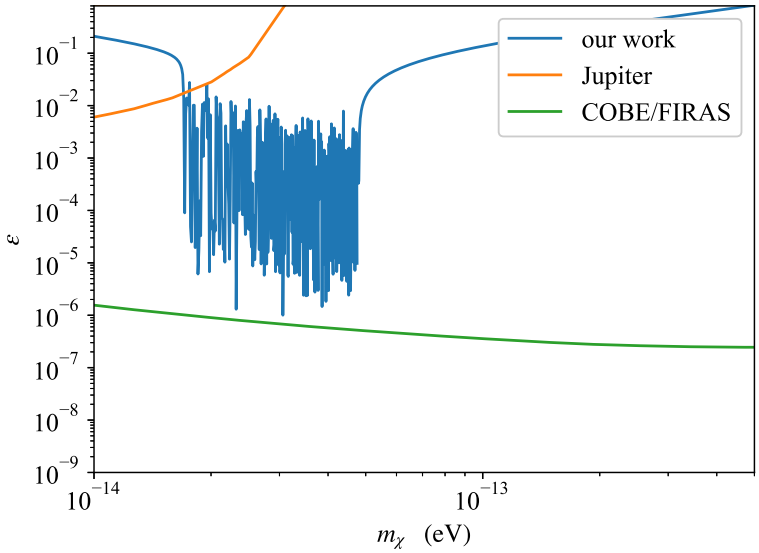

Figure 2. The sensitivity of this quasar lensing-based dark photon detection scheme. The blue solid line represents our method's sensitivity, which complements existing constraints; the orange solid line shows limits from the Jupiter magnetic field experiment [33,34] and the green solid line indicates COBE/FIRAS [9–12,35] bounds on CMB spectral distortions.

Relative to the Jupiter magnetic experiment [33,34] and COBE/FIRAS [9–12,35], our method do not achieve improved sensitivity. Future advancements in data analysis algorithms or observational precision could enhance sensitivity. If radio waveband observations are employed, Equation (27) indicates that the detection sensitivity improves as E_γ decreases.

The gravitational lensing approach can also constrain the dark photon parameter space by leveraging the gravitational bending of AGN radio wavebands by the Sun, as discussed in the framework by Lobanov et al. [32]. For Type Ia supernovae exhibiting gravitational lensing effects, their theoretically identical intrinsic luminosities allow the precise determination of luminosity attenuation, granting this method a distinct advantage. Additionally, in mutually orbiting compact object star binary systems with well-characterized observational data, our proposed scheme could be applied to derive constraints on dark photons.

While the gravitational lensing scheme cannot fully exploit the mass-independent nature of photon–dark photon oscillations in gravitational fields, we propose that neutron star evolution and black hole accretion disk systems may exhibit more pronounced signatures of gravitationally induced dark photon decoherence. These systems, characterized by extreme gravitational fields and high-energy environments, offer unique opportunities to probe dark photon interactions. However, their complex dynamics and emission mechanisms require detailed modeling to disentangle dark photon effects from astrophysical backgrounds.

5. Conclusions and Prospects

We propose a novel oscillation mechanism between photon and dark photon mass eigenstates during propagation in media under gravitational fields, deriving the oscillation probability formula. Unlike conventional dark photon detection schemes, this mechanism is immune to medium-induced suppression of oscillations. Furthermore, we suggest that gravity can induce photon–dark-photon mass-state separation during their propagation through interstellar media. By observing the potential attenuation in gravitationally lensed

quasar luminosities, we seek to constrain the dark photon parameter space. Under typical system-scale assumptions, our preliminary estimate indicates that for dark photon masses in the range 1.7×10^{-14} eV to 5.4×10^{-14} eV, the sensitivity to the mixing parameter ε can reach approximately 10^{-2}. This result can be further improved with additional data and a more detailed analysis. Finally, we anticipate that this oscillation mode may be fruitfully exploited in neutron star and black hole accretion disk systems.

Author Contributions: Conceptualization, B.Z. and C.-B.L.; methodology, B.Z.; software, B.Z.; validation, B.Z.; formal analysis, B.Z.; investigation, B.Z.; resources, B.Z.; data curation, B.Z.; writing—original draft preparation, B.Z.; writing—review and editing, B.Z.; visualization, B.Z.; supervision, C.-B.L.; project administration, C.-B.L.; funding acquisition, B.Z. All authors have read and agreed to the published version of the manuscript.

Funding: This research received no external funding.

Data Availability Statement: No new data were created or analyzed in this study.

Conflicts of Interest: The authors declare no conflict of interest.

Abbreviations

The following abbreviations are used in this manuscript:

SM	Standard Model
BSM	beyond-the-Standard-Model
CMB	cosmic microwave background
LSW	light-shining-through-wall experiment
AGN	active galactic nucleus

Appendix A. Deflection Angle Between Photon and Dark Photon

Appendix A.1. Calculation Basis

This appendix presents calculation process of the gravitational lensing deflection angle of a massive particle and massless particle. Firstly, the gravity of the foreground is described by the Schwarzschild metric with isotropic static, assuming

$$ds^2 = g_{\mu\nu}dx^\mu dx^\nu = -(1-\frac{2M}{r})dt^2 + (1-\frac{2M}{r})^{-1}dr^2 + r^2d\theta^2 + r^2\sin^2\theta d\phi^2. \tag{A1}$$

The Lagrangian can be written as

$$\begin{aligned} L_G = -\frac{1}{2}g_{\mu\nu}\dot{x}^\mu\dot{x}^\nu &= \frac{1}{2}(1-\frac{2M}{r})(\frac{dt}{d\lambda})^2 + (1-\frac{2M}{r})^{-1}(\frac{dr}{d\lambda})^2 \\ &\quad + r^2(\frac{d\theta}{d\lambda})^2 + r^2\sin^2\theta(\frac{d\phi}{d\lambda})^2, \end{aligned} \tag{A2}$$

where λ is affine parameter, which could be defined as proper time for the massive particle. The Lagrangian is based on the four-velocity of the particle, thus

$$L_G = \kappa = \begin{cases} 0 & (massless \quad particle) \\ \frac{1}{2} & (massive \quad particle) \end{cases}. \tag{A3}$$

The isotropic and static condition suggest two first integrals

$$\frac{\partial L_G}{\partial t} = 0, \qquad \frac{\partial L_G}{\partial \phi} = 0. \tag{A4}$$

This means two conserved quantities: energy and angular momentum. red

$$\begin{aligned} E =& \frac{\partial L_G}{\partial \dot{t}} = (1 - \frac{2M}{r}) \frac{dt}{d\lambda}, \\ L =& \frac{\partial L_G}{\partial \dot{\phi}} = r^2 \sin^2 \frac{d\phi}{d\lambda}. \end{aligned} \tag{A5}$$

Combining Equations (A2) and (A3), we obtain normalization condition of four-velocity.

$$\left(\frac{dr}{d\lambda}\right)^2 = E^2 - (1 - \frac{2M}{r})(2\kappa - \frac{L^2}{r^2}). \tag{A6}$$

The calculation is based on Equations (A5) and (A6) and would be divided into a massive section and massless section.

Appendix A.2. Deflection of Massless Particle (Photon)

This section discusses the massless particle deflection in gravity. Set $\kappa = 0$, reduce λ and obtain the orbital equation by combining Equations (A5) and (A6).

$$\left[\frac{d}{d\phi}(\frac{1}{r})\right]^2 = \left[\frac{E}{L}\right]^2 - \frac{1}{r^2}(1 - \frac{2M}{r}). \tag{A7}$$

Equation (A7)'s derivation of ϕ can be simplified as

$$\frac{d^2u}{d\phi^2} + u = 3Mu^2, \tag{A8}$$

where $u = 1/r$. Equation (A8) and the original conditions contain the orbit information of the massless particle. The last task is solving the differential equation. The nonlinear feature makes it hard. The nonlinear term is contributed to by gravity. As gravity is small in a gravitational lensing system, the term $3Mu^2$ is regarded as a perturbation. The solution of Equation (A8) is

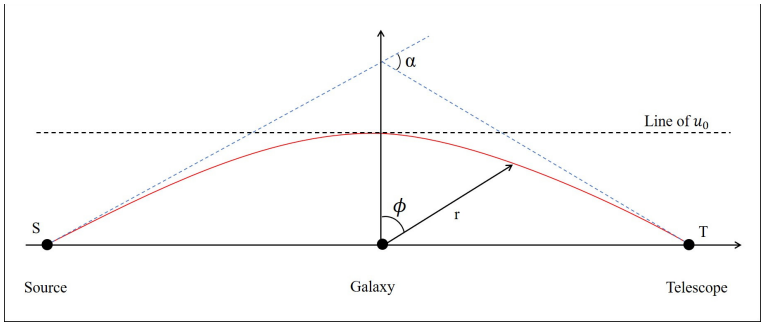

Figure A1. Illustration of parameters of massless and massive particle geodesic.

$$u = u_0 + \xi u_1 + o(\xi^2), \qquad where \quad \xi = 3M. \tag{A9}$$

Substituting Equation (A9) into Equation (A8), we have

$$\frac{d^2u_0}{d\chi^2} + u_0 = 0, \tag{A10a}$$

$$\frac{d^2u_1}{d\chi^2} + u_1 = u_0^2. \tag{A10b}$$

Equation (A10a) describes a scene without gravity, so the solution is

$$u_0 = \frac{\cos\phi}{R_{galaxy}}. \tag{A11}$$

Hence, the first order approximate solution of Equation (A8) is

$$u = \frac{\cos\phi}{R_{galaxy}} + \frac{M}{R_{galaxy}^2}(1+\sin^2\phi). \tag{A12}$$

Limiting r to infinity, $u \to 0$, Equation (A11) suggests $\phi' = \pm\pi/2$. The deflection angle in the first order approximation Equation (A12) can be defined as

$$\phi = \phi' \pm \alpha' = \pm(\frac{\pi}{2} + \alpha'). \tag{A13}$$

α' is a half of total deflection angle. Equations (A12) and (A13) derive the deflection angle of photon in a gravitational field.

$$\alpha_{massless} = 2\alpha' = \frac{4M}{R_{galaxy}} = \frac{4GM}{R_{galaxy}c^2}. \tag{A14}$$

Appendix A.3. Deflection of Massive Particle

In this section, we focus on massive particle orbital character in gravity. Set $\kappa = 1/2$, follow Equations (A7) and (A8), and we have

$$\frac{d^2u}{d\phi^2} + u = \frac{M}{L^2} + 3Mu^2. \tag{A15}$$

We concern the low mass range of DP in order to obtain a lower undetectable mass limit for our work. M/L^2 is bigger than $3Mu^2$ in classical physics. But for a small mass condition, the state is reversed. M/L^2 needs to be regarded as a first order approximation at least. Using the same perturbation strategy, the solution to Equation (A11) is also the zeroth-order approximation solution of Equation (A15). Taking Equation (A11) into Equation (A15) gives

$$\frac{d^2u_1}{d\phi^2} + u_1 = \frac{M}{L^2} + 3M\left(\frac{\cos\phi}{R_{galaxy}}\right)^2. \tag{A16}$$

Its solution is under the first order approximation, showing as

$$u_1 = \frac{M}{L^2} + \frac{M}{R_{galaxy}^2}(1+\sin^2\phi). \tag{A17}$$

So, the solution of Equation (A15) in the first order approximation is

$$u = \frac{\cos\phi}{R_{galaxy}} + \frac{M}{L^2} + \frac{M}{R_{galaxy}^2}(1+\sin^2\phi). \tag{A18}$$

Deflection angle α'' can be defined in

$$\phi = \pm(\frac{\pi}{2} + \alpha''). \tag{A19}$$

We could obtain the total deflection angle by combining this with Equation (A19) and $u = 0$.

$$\alpha_{massive} = 2\alpha'' = \frac{2MR_{galaxy}}{L^2} + \frac{4M}{R_{galaxy}}. \tag{A20}$$

L corresponds to angle momentum of per rest mass,

$$L = \frac{\vec{r} \times \vec{p}}{m_0} = \frac{R_{galaxy} m\beta}{m_0} = \frac{\beta}{\sqrt{1-\beta^2}} R_{galaxy}, \tag{A21}$$

where $\beta = v/c$. Therefore,

$$\alpha_{massive} = \frac{2M}{R_{galaxy}\beta^2} + \frac{2M}{R_{galaxy}} = \frac{2GM}{R_{galaxy}v^2} + \frac{2GM}{R_{galaxy}c^2}. \tag{A22}$$

Appendix A.4. The Differential Angular Deflection

The differential angular deflection can be derived by taking the difference between Equations (A22) and (A14):

$$\Delta\alpha = \frac{2GM}{R_{galaxy}c^2}\left(\frac{m_\chi^2}{E^2 - m_\chi^2}\right). \tag{A23}$$

References

1. Feng, L.; Yang, R.Z.; He, H.N.; Dong, T.K.; Fan, Y.Z.; Chang, J. AMS-02 positron excess: New bounds on dark matter models and hint for primary electron spectrum hardening. *Phys. Lett. B* **2014**, *728*, 250–255.
2. Holdom, B. Two U (1)'s and epsilon charge shifts. *Phys. Lett. B* **1986**, *166*, 196–198.
3. Okun, L.B. *Limits of Electrodynamics: Paraphotons*; Technical Report; Gosudarstvennyj Komitet po Ispol'zovaniyu Atomnoj Ehnergii SSSR: Moscow, Russia, 1982.
4. Redondo, J. Helioscope bounds on hidden sector photons. *J. Cosmol. Astropart. Phys.* **2008**, *2008*, 8.
5. Barducci, D.; Bertuzzo, E.; Grilli di Cortona, G.; Salla, G.M. Dark photon bounds in the dark EFT. *J. High Energy Phys.* **2021**, *2021*, 1–20. [CrossRef]
6. Jaeckel, J.; Redondo, J.; Ringwald, A. Signatures of a hidden cosmic microwave background. *Phys. Rev. Lett.* **2008**, *101*, 131801. [CrossRef]
7. Danilov, M.; Demidov, S.; Gorbunov, D. Constraints on hidden photons produced in nuclear reactors. *Phys. Rev. Lett.* **2019**, *122*, 041801.
8. An, H.; Pospelov, M.; Pradler, J. New stellar constraints on dark photons. *Phys. Lett. B* **2013**, *725*, 190–195.
9. Mirizzi, A.; Redondo, J.; Sigl, G. Microwave background constraints on mixing of photons with hidden photons. *J. Cosmol. Astropart. Phys.* **2009**, *2009*, 26.
10. McDermott, S.D.; Witte, S.J. Cosmological evolution of light dark photon dark matter. *Phys. Rev. D* **2020**, *101*, 063030. [CrossRef]
11. Caputo, A.; Liu, H.; Mishra-Sharma, S.; Ruderman, J.T. Dark photon oscillations in our inhomogeneous universe. *Phys. Rev. Lett.* **2020**, *125*, 221303.
12. García, A.A.; Bondarenko, K.; Ploeckinger, S.; Pradler, J.; Sokolenko, A. Effective photon mass and (dark) photon conversion in the inhomogeneous Universe. *J. Cosmol. Astropart. Phys.* **2020**, *2020*, 011.
13. Ahlers, M.; Gies, H.; Jaeckel, J.; Redondo, J.; Ringwald, A. Laser experiments explore the hidden sector. *Phys. Rev. D—Part. Fields Gravit. Cosmol.* **2008**, *77*, 095001.
14. Redondo, J.; Raffelt, G. Solar constraints on hidden photons re-visited. *J. Cosmol. Astropart. Phys.* **2013**, *2013*, 034.
15. An, H.; Pospelov, M.; Pradler, J.; Ritz, A. Direct detection constraints on dark photon dark matter. *Phys. Lett. B* **2015**, *747*, 331–338.
16. Liu, X.H.; Li, Z.H.; Qi, J.Z.; Zhang, X. Galaxy-scale test of general relativity with strong gravitational lensing. *Astrophys. J.* **2022**, *927*, 28.
17. Reyes, R.; Mandelbaum, R.; Seljak, U.; Baldauf, T.; Gunn, J.E.; Lombriser, L.; Smith, R.E. Confirmation of general relativity on large scales from weak lensing and galaxy velocities. *Nature* **2010**, *464*, 256–258.
18. Grespan, M.; Biesiada, M. Strong gravitational lensing of gravitational waves: A review. *Universe* **2023**, *9*, 200. [CrossRef]
19. Osłowski, S.; Moderski, R.; Bulik, T.; Belczynski, K. Gravitational lensing as a probe of compact object populations in the Galaxy. *Astron. Astrophys.* **2008**, *478*, 429–434.

20. Wen, D.; Kemball, A.J. Testing Primordial Black Hole Dark Matter with Atacama Large Millimeter Array Observations of the Gravitational Lens B1422+ 231. *Universe* **2024**, *10*, 37. [CrossRef]
21. Zumalacarregui, M.; Seljak, U. Limits on stellar-mass compact objects as dark matter from gravitational lensing of type Ia supernovae. *Phys. Rev. Lett.* **2018**, *121*, 141101.
22. Swami, H.; Lochan, K.; Patel, K.M. Signature of neutrino mass hierarchy in gravitational lensing. *Phys. Rev. D* **2020**, *102*, 024043. [CrossRef]
23. Glicenstein, J.F. Gravitational lensing of photons coupled to massive particles. *Phys. Rev. D* **2018**, *97*, 083005. [CrossRef]
24. Fomalont, E.; Kopeikin, S.; Lanyi, G.; Benson, J. Progress in measurements of the gravitational bending of radio waves using the VLBA. *Astrophys. J.* **2009**, *699*, 1395. [CrossRef]
25. Park, H. Detecting dark photons with reactor neutrino experiments. *Phys. Rev. Lett.* **2017**, *119*, 081801. [CrossRef]
26. An, H.; Pospelov, M.; Pradler, J. Dark matter detectors as dark photon helioscopes. *Phys. Rev. Lett.* **2013**, *111*, 041302. [CrossRef] [PubMed]
27. Donges, A. The coherence length of black-body radiation. *Eur. J. Phys.* **1998**, *19*, 245. [CrossRef]
28. Gaston, B. Luminosity function of high-redshift quasars. *Astrophys. J.* **1983**, *272*, 411–433. [CrossRef]
29. Notini, P.; Richter, G. Luminosity Functions of Quasars and Seyfert Galaxies. *Astron. Nachrichten* **1972**, *294*, 95–104. [CrossRef]
30. Pei, Y.C. The luminosity function of quasars. *Astrophys. J.* **1995**, *438*, 623–631. [CrossRef]
31. Hawkins, M.; Veron, P. The evolution of the quasar luminosity function. *Mon. Not. R. Astron. Soc.* **1995**, *275*, 1102–1116. [CrossRef]
32. Lobanov, A.P.; Zechlin, H.S.; Horns, D. Astrophysical searches for a hidden-photon signal in the radio regime. *Phys. Rev. D—Part. Fields Gravit. Cosmol.* **2013**, *87*, 065004.
33. Marocco, G. Dark photon limits from magnetic fields and astrophysical plasmas. *arXiv* **2021**, arXiv:2110.02875.
34. Yan, S.; Li, L.; Fan, J. Constraints on photon mass and dark photon from the Jovian magnetic field. *J. High Energy Phys.* **2024**, *2024*, 28. [CrossRef]
35. Fixsen, D.J.; Cheng, E.; Gales, J.; Mather, J.C.; Shafer, R.; Wright, E. The cosmic microwave background spectrum from the full cobe* firas data set. *Astrophys. J.* **1996**, *473*, 576. [CrossRef]